
**Impact and implications of climate
variability and change on glacier mass
balance in Kenya**

**University of Reading
Department of Mathematics, Meteorology and Physics.**

Neeral Shah

A dissertation submitted in partial fulfilment of the requirement for the
degree of MSc in *Mathematical and Numerical Modelling of the
Atmosphere and Ocean*

Declaration

I confirm that this is my own work and the use of all material from other sources has been properly and fully acknowledged.

Neeral Shah

Abstract

Kenya's economy relies heavily on the agricultural industry as its main source of economy. Glaciers provide a large store of freshwater and modelling of the meltwater associated with this is of great interest to water management. With growing concern over the impact of glacier retreat on runoff and streamflow, this study aims to simulate runoff from the tropical Lewis Glacier in Central Kenya and its impacts on runoff due to climate variability.

Acknowledgments

The writing of this dissertation has been one of the most significant academic challenges I have ever had to face. Without the support, patience and guidance of the following people, this study would not have been completed. It is to them I owe everlasting gratitude.

- To Professor Nigel Arnell, thank you for undertaking the role of being my supervisor and the duties associated with it. I have enjoyed working with you.
- To the Mathematics and Meteorology departments at the University of Reading, without whom this study would not have been possible. Special thanks goes to Professor Mike Baines and Sue Davis for always being there and giving a word or two of encouragement to keep us going.
- To Mr Simon Gosling, thank you for all the data sets you provided me without which this project would not have been possible and the open door policy you shared.
- To Rashmita and Jayendra Shah, you mean the world to me. Thank you for supporting me and believing in all my endeavours.
- To Ankeet Shah, thank you for being my one of my sources of inspiration.
- To Jasdeep Giddie, thank you for all your love and patience, for believing in me and most of all, for all the compromises you have had to make this year so I could undertake this task.

'Asante Sana' to all friends and family who have taken this journey with me.

Contents

Acknowledgements	i
1 Introduction	1
1.1 Background	1
1.2 Goals	3
1.3 Outline	3
2 Experimental Design	4
2.1 The Study Approach	4
2.2 The Lewis Glacier Model	5
2.3 The Hydrological Model - Mac-PDM	6
2.4 Emission Scenarios Data Sets	10
3 The Lewis Glacier Model	11
3.1 Background	11
3.2 Some Definitions	12
3.3 The Model	13
3.4 Stability and Accuracy	17
4 Results and Analyses	19
4.1 Modelled Mass Balance Profile of the Lewis Glacier	19

<i>CONTENTS</i>	iv
4.2 Mass Balance and Volume of Glacier	20
4.3 Implications of Surface Runoff and Glacier Melt	20
4.4 Climate variability and Runoff	21
5 Discussion and Summary	31
5.1 Caveats	31
5.2 Conclusion	32
5.3 Further Work	33
Bibliography	33

Chapter 1

Introduction

1.1 Background

Kenya relies heavily on its natural resources to generate income. High altitude, fertile soils and abundance of precipitation (1000mm) in Central and Western Kenya make it the ideal place for growing tea and coffee, two of Kenya's highest GDP earners. Other agricultural goods such as horticulture and sugar cane also rely heavily on water availability. The impacts on water resources in Kenya due to climate variability are thus of great importance.

Mount Kenya is located on the equator in East Africa with the two highest peaks, Batian and Nelion, reaching about 5,200 m. It lies at the apex of three water sheds, Uasin Nyiro, Tana and Rift Valley catchments as per the map below. According to Young & Hastenrath (1991), there are total of 11 glaciers on Mount Kenya, of which the Lewis and Tyndall glaciers are the two largest and most studied. In this study, the focus will be on the modelling of the mass balance of the Lewis Glacier as it covers the largest area of 0.31 km².

In high mountainous catchments, glaciers represent the most important water storage reservoir. Thus glacier mass balance estimated over long periods of time is a good indicator of the overall water balance of the catchment (Schaeffli *et al.* (2005)). The idea of mass balance is an important link between climatic inputs and and glacier behaviour and as a result future water

balance can be predicted for catchments containing advancing or retreating glaciers (Bienn and Evans (1998)).

1.2 Goals

The aims of this study are:

1. To model the mass balance profile of the Lewis Glacier using baseline and climate change data; and
2. To assess the effects of the change in glacier mass balance on downstream water resources

1.3 Outline

The outline of the dissertation is as follows:

In the second chapter the study approach, an introduction to the glacier model, the hydrological model and data sets used are discussed.

In Chapter 3, the glacier model based on Kaser (2001) and Kaser and Osmaston (2002) is developed.

Results of the study are presented in Chapter 4.

Finally, Chapter 5 summarises the findings of the study along with caveats and further work is proposed.

Chapter 2

Experimental Design

This is the chapter where I describe the models and data sets used.

1. Glacier model
2. Mac-PDM model
3. Data Basis

2.1 The Study Approach

The approach to the study on the effects of the Lewis Glacier on the hydrological system in Kenya was as follows:

1. Develop a mass balance profile to evaluate the amount of water (and hence runoff) held on the Lewis Glacier, Mount Kenya using baseline and climatic data;
2. Convert mass balance into runoff by determining the volume of the glacier and hence meltwater;
3. Compare the performance of the system between baseline and altered climate inputs and between mass balance profiles and non mass balance profiles with baseline and altered climate inputs.

4. Run the ‘Mac-PDM’ global hydrological model to simulate streamflow in Kenya with baseline and climatic data;
5. Compare simulated runoff from the glacier and hydrological models and note any impacts the glacier retreat may have on the catchment.

2.2 The Lewis Glacier Model

Glaciers account for 75% of the world’s fresh water. Of these, the tropics account for 0.15% of global glacier area and hence freshwater sources.

Glaciers are an important part of the hydrological cycle as they act as an intermediate store, regulating the seasonal and long-term runoff variations on the highest of mountain ranges (Kaser *et al.* (2003)). In addition, mountainous regions are good sources of water supply as they enhance convective precipitation due to their orographic features.

Hydrological models that are able to simulate runoff from snow and ice melt affected catchments are particularly useful to predict floods due to sudden release of meltwater, water flow rate for hydro power dams located in mountainous regions, and sources of freshwater supply for domestic, agricultural and industrial purposes.

The modelling of the Lewis Glacier is based on calculation of the mass balance using the vertical profile of specific mass balance (VBP) method proposed by Kaser (2001) and Kaser and Osmaston (2002) which shall be discussed in more detail in Chapter 3. This method involves seeking the vertical mass balance gradient (variation of the mass budget with altitude) in consideration of the vertical gradients of accumulation, air temperature, albedo, the duration of the ablation period and a factor for the ratio between melting and sublimation of the glacier.

The Glacier Model and the Hydrological Model

The glacier model outlined above is used to calculate the specific mass balance profile of a defined glacier in [kg m^{-2}] in terms of its vertical accumula-

tion and ablation gradients. The mass balance profile is proportional to the size of the glacier and hence we can estimate the volume of water stored in the glacier may be estimated. Converting the glacier into the water equivalent, the meltwater runoff can be added to average runoff in each grid cell that the glacier occurs in.

2.3 The Hydrological Model - Mac-PDM

Background

A macro-scale model is one which can be applied repeatedly over a large geographic domain and does not need to be calibrated at the catchment scale. According to Arnell (1999a), the model was first developed to be used by hydrologists to simulate the effects of climate change in East Africa (Arnell (1999b)), where observed data is scarce, and later extended to cover the whole world.

The hydrological model was used to simulate runoff in Kenya using Climatic Research Unit (CRU) dataset for present day data from 1961 - 1990, while climate change projections came from 5 different models, CCMA-CGCM31, IPSL-CM4, MPI-ECHAM5, NCAR-CCSM30 and UKMO-HADCM3 using the A1B emission scenario from the International Panel on Climate Change (IPCC) 1997 reports.

Mac-PDM Hydrological Model

The Mac-PDM Model as explained by Arnell (1999a, 2003) is described below.

The hydrological model used is a conceptual water balance model working on a time step of one day, with the following basic structure:

$$\frac{dS}{dt} = P - E - D - Q$$

where P , E , D and Q are precipitation, evaporation, delayed run off and direct runoff during the time interval t , respectively. dS is the change in storage of water in soil, lakes and wetlands over the time t .

Streamflow is simulated at a spatial resolution of $0.5 \times 0.5^\circ$ (or 2000 km^2), treating each grid cell as an independent catchment. Input parameters are assumed to be constant across the entire grid cell while soil moisture storage capacity varies with a statistical distribution across the grid cell. The model parameters have not been calibrated from site data, but the performance of the model has been validated and found that it simulates average annual runoff reasonably well (Arnell, 1999a, 2003). The hydrological model currently does not simulate melt water from glacierized areas.

The model differentiates precipitation as snow if temperature is below a defined threshold and rain otherwise. Snow melts once temperature reaches another threshold. Precipitation is intercepted by vegetation until the interception capacity has been reached, the excess falling to the ground. Precipitation that has not been intercepted or on the ground is evaporated.

Potential evaporation is calculated using the Penman-Monteith formula:

$$E = \frac{1000}{\lambda \rho_w} \left[\frac{\Delta R_n + 86.4 \rho_a c_p (e_s - e) / r_a}{\Delta + \gamma [1 + r_s / r_a]} \right]$$

where λ is the latent heat of vapourisation, ρ_w is density of water, ρ_a is density of air, Δ is gradient of the relationship between vapour pressure and temperature, R_n is net radiation, c_p is specific heat capacity of the air, e_s is saturated vapour pressure, e is vapour pressure, r_a is aerodynamic resistance, r_s is surface resistance and γ , is the psychrometric constant. The aerodynamic resistance and surface resistance are dependent on vegetation type and thus each grid cell is divided into either 'grass' or 'not grass' vegetation type. Characteristics of 'not grass' vary from cell to cell based on the land cover data taken from the global land cover data set produced by deFries *et al.* (1998). Each part of the cell has the same inputs and soil properties and the output of the two parts is summed to give a total cell response.

If the soil is saturated, water that reaches the ground becomes 'quickflow', and infiltrates the soil otherwise. Soil moisture is depleted by evaporation and drainage to a deep store ('slowflow') when soil moisture storage is above field capacity. A variable proportion of the grid cell is saturated at any one time generating 'quickflow' from this proportion of the cell. This is

achieved by statistically varying the soil moisture storage capacity in each grid cell.

Actual evaporation (AE) is a linear function of potential evaporation (PE) and average cell soil moisture content. When field capacity (FC) is reached, actual evaporation is less than the potential evaporation and can be summarised as

$$\begin{aligned} \frac{AE}{PE} &= 1 & S_t &\geq FC, \\ \frac{AE}{PE} &= \frac{S_t}{FC} & S_t &\leq FC. \end{aligned}$$

Quickflow (direct runoff) and slowflow (delayed runoff) are routed separately to the outlet of the grid cell to generate streamflow. Direct runoff is routed through two parallel linear reservoirs to create streamflow. The streamflow contribution from delayed runoff is assumed to be a non-linear function of the amount of water held in groundwater and deep soil store. Water is not routed from cell to cell since the aim of the simulations is to simulate the change in spatial pattern of streamflow and not at specified points along a river system.

Table 2.1 summarises the parameters used in the hydrological model.

Parameter	Description	Source
T_{crit}	Temperature threshold for snowfall and snowmelt	0° C - Fixed
Melt	Melt rate	4 mm °C ⁻¹ d ⁻¹) Fixed
b	Parameter describing distribution of soil moisture capacity	0.25 Fixed
Sat	Saturation capacity in %	Function of soil texture and vegetation
FC	Field capacity in %	Function of soil texture and vegetation
RFF	fraction of cell that is not "not grass"	Function of vegetation type
γ	Interception capacity	Function of vegetation type
δ	Parameters of interception model	Fixed
Root depth	Depth of vegetation used to define saturation and field capacity in absolute terms	Function of vegetation type
LAI	Leaf area index used in Penman-Monteith	Function of vegetation type
r_s	Stomatal conductance used in Penman-Monteith	Function of vegetation type
H_c	Vegetational roughness height used in Penman-Monteith	Function of vegetation type
S_{rout}	Routing parameter for direct runoff	Fixed
G_{rout}	Routing parameter for delayed runoff	Fixed

Each grid cell is classified according to a soil type based on United Nations Food and Agriculture (FOA) data. Soil type is important as soil moisture storage is a function of texture.

To account for variations in seasons, a sine curve is fitted to maximum and minimum monthly temperatures with an additional random deviation of 2° around the sine curve to simulate fluctuations in daily temperature.

2.4 Emission Scenarios Data Sets

The climate change data is based upon the pattern scaling technique. The scenarios have been developed using ClimGen. The data for 5 GCMs, for the A1B emissions scenario, for 2040-2069. The scenarios used are for the patterns of climate change associated with 5 different General Circulation Models (GCM). The 5 models are (modelling institution and model version):

- IPSL CM4
- CCCMA CGCM31
- UKMO HadCM3
- MPI ECHAM5
- NCAR CCSM30

The A1B scenario family describes a future world of very rapid economic growth, global population that peaks in mid-century and declines thereafter, and the rapid introduction of new and more efficient technologies. Major underlying themes are convergence among regions, capacity building and increased cultural and social interactions, with a substantial reduction in regional differences in per capita income. The A1 scenario family develops into three groups that describe alternative directions of technological change in the energy system. The three A1 groups are distinguished by their technological emphasis: fossil intensive (A1FI), non-fossil energy sources (A1T), or a balance across all sources (A1B) (where balanced is defined as not relying too heavily on one particular energy source, on the assumption that similar improvement rates apply to all energy supply and end-use technologies) (UNEP, 2001)

Chapter 3

The Lewis Glacier Model

3.1 Background

Modelling of glaciers (prediction of meltwater driven streamflow) has been regarded as a valuable tool for efficient water resource management. As a result, several models have been developed. According to Hock (2005), the range of models used to forecast meltwater production from glaciers ranges from energy-balance models to temperature-index models and several mixtures of the two.

Glaciers can be classed into three broad categories, each with unique characteristics: polar glaciers, midlatitude glaciers and tropical glaciers. Tropical glaciers can be further divided into inner tropics and outer tropics (Kaser and Osmaston, 2002).

Tropical glaciers have gained increased attention in the context of global change due to their role in regional water budgets (Hastenrath, 1995). Glaciers still exist near the Equator in Africa (Mount Kilimanjaro, Mount Kenya, Ruwenzori Mountains), South America (South America Andes) and New Guinea (Irian Jaya), but have begun to retreat rapidly since the 19th century.

According to Innes (2009) the limits of the tropics are defined where

1. the sun is directly overhead at some point in the year (23° N - 23°);

2. the region experiences net heating: incoming solar radiation is greater than outgoing terrestrial radiation;
3. sea surface temperatures exceed 24° C; and
4. the diurnal cycle of temperature exceeds the annual cycle (no seasonal variation except for oscillating ‘wet’ and ‘dry’ periods defined by precipitation).

Mount Kenya thus clearly falls within the tropics and the glacier modelled accordingly.

Mass Balance can be measured in one of four ways:

1. Direct measurements from ice cores
2. Remote Sensing methods
3. Hydrological methods using formulas such as:

$$B_n = P - R - E$$

where B_n is net balance, P is precipitation, R is runoff and E is evaporation.

4. Climatic calculations from meteorological data using measurement and estimates of precipitation, radiation flux, temperature and other factors in the energy balance calculations (Bienn and Evans (1998)).

3.2 Some Definitions

The mass balance (or mass budget) of a glacier is defined as the difference between gains (accumulation) and losses (ablation), expressed in terms of water equivalent [kg m⁻²], measured over a specified time period, usually one year. The annual net mass balance is defined as the net change (sum of annual accumulation and annual ablation (negative)) in glacier mass between the same date in successive years.

The amount of annual ablation and accumulation varies systematically with altitude. The rate at which annual ablation and accumulation change with altitude are termed ablation gradient and accumulation gradient, respectively. Together they define the mass balance gradient.

Mass balance gradients link climatic conditions on ablation and accumulation with glacier behaviour and is therefore an important measure of glacier activity (Bienn and Evans, 1998). Ablation gradients vary approximately linearly with altitude, being highest at the snout and decreasing with altitude because temperature declines with higher altitude at a lapse rate of 0.0065 K m^{-1} . Conversely, accumulation generally increases with altitude, rising from zero at the equilibrium line (ELA). ELA is the altitude at which ablation is equal to accumulation and hence net mass balance is zero. According to Kaser (2001) and Kaser and Osmaston (2002), the ELA is more or less equal to the altitude at which the air temperature is 0° C at the inner tropics.

3.3 The Model

The model described below is based on the vertical mass balance gradient compiled by Kuhn (1980) and further developed by Kaser (2001) and Kaser and Osmaston (2002).

The specific mass budget b at any altitude z on a glacier over a specific period, usually one year, is made up of the sum of specific accumulation $c(z)$ and specific ablation $a(z)$

$$b(z) = c(z) + a(z). \quad (3.1)$$

This is also true for the vertical mass balance gradient

$$\frac{db}{dz} = \frac{\partial c}{\partial z} + \frac{\partial a}{\partial z} \quad (3.2)$$

with $c(z)$ positive, $a(z)$ negative and z positive vertically upward.

Ablation is made up of meltwater runoff $m(z)$ and the sublimation process $s(z)$ into the atmosphere, Both are governed by latent heat fluxes $Q_M(z)$ for melting and $Q_L(z)$ for sublimation. Thus specific ablation is

$$a(z) = m(z) + s(z) = \tau(z) \left(\frac{1}{L_M} Q_M(z) + \frac{1}{L_S} Q_L(z) \right) \quad (3.3)$$

with the heat of fusion $L_M = 0.334$ in $[\text{MJ kg}^{-1}]$, the heat of sublimation $L_S = 2.835$ in $[\text{MJ kg}^{-1}]$, and the duration of the ablation season τ , counted in days [d].

The heat balance on the surface of the glacier is given by

$$Q_M(z) + Q_L(z) + Q_R(z) + Q_S(z) = 0 \quad [\text{MJ m}^{-2} \text{d}^{-1}] [\text{MJ m}^{-2} \text{d}^{-1}] [\text{MJ m}^{-2} \text{d}^{-1}] [\text{MJ m}^{-2} \text{d}^{-1}] \quad (3.4)$$

where $Q_R(z)$ is the heat flux resulting from the radiation balance and $Q_S(z)$ is the sensible heat flux. If $Q_M(z)$ is replaced with the help of (3.4), then specific ablation becomes

$$a(z) = -\tau(z) \left[\frac{1}{L_M} (Q_R(z) + Q_S(z)) + \left(\frac{1}{L_S} - \frac{1}{L_M} \right) Q_L(z) \right] \quad (3.5)$$

The sensible heat flux $Q_S(z)$ is derived from the heat transfer coefficient for turbulent exchange α_s in $[\text{MJ m}^{-2} \text{d}^{-1} \text{ } ^\circ\text{C}^{-1}]$ and the difference in temperature between the atmosphere and the surface of the glacier ($T_a(z) - T_s(z)$) in [K]

$$Q_S(z) = \alpha_s (T_a(z) - T_s(z)). \quad (3.6)$$

The radiation balance is composed of the absorbed portion of the global (shortwave) radiation $G(z)(1 - r(z))$, the atmospheric incoming longwave radiation $A(z)$ and the outgoing longwave radiation $E(z)$,

$$\begin{aligned} Q_R(z) &= G(z)(1 - r(z)) + A(z) + E(z) \\ &= G(z)(1 - r(z)) + \varepsilon_a \sigma T_a(z)^4 - \varepsilon_s \sigma T_s(z)^4, \end{aligned} \quad (3.7)$$

where ε_a and ε_s are emission coefficients of the atmosphere near the surface and the surface of the glacier, respectively. Together with the Stefan-Boltzman constant $\sigma = 4.9 \times 10^{-9}$ $[\text{MJ m}^{-2} \text{d}^{-1} \text{ K}^4]$, ε_a and ε_s are used to calculate the incoming and outgoing longwave radiation from climatic data.

Thus, the specific ablation is

$$\begin{aligned} a(z) = -\tau(z) & \left\{ \frac{1}{L_M} [G(z)(1 - r(z)) + \varepsilon_a \sigma T_a(z)^4 - \varepsilon_s \sigma T_s(z)^4 + \alpha_s (T_a(z) - T_s(z))] \right. \\ & \left. + \left(\frac{1}{L_S} - \frac{1}{L_M} \right) Q_L(z) \right\} \end{aligned} \quad (3.8)$$

Taking a reference level z_{ref} where $T_a = 273.15 \text{ K} = 0^\circ\text{C}$, which is equal to the 0°C level during the ablation period and taking into account the following assumptions:

- the surface temperature $T_s = 273.15 \text{ K} = 0^\circ\text{C}$ over the entire glacier,
- the vertical gradient of the effective global radiation is $\partial G(1-r)/\partial z = 0$, and
- the vertical gradient of the latent heat flux is $\partial Q_L/\partial z = 0$,
- $4\varepsilon_a\sigma 273.15^3 = \alpha_R$

then the vertical ablation gradient at z_{ref} is

$$\begin{aligned} \frac{\partial a}{\partial z}\Big|_{z_{ref}} = & -\frac{\partial \tau}{\partial z} \left\{ \frac{1}{L_M} [G(1-r) + \varepsilon_a\sigma T_a^4 - \varepsilon_s\sigma T_s^4 + \alpha(T_a - T_s)] \right. \\ & \left. + \left(\frac{1}{L_S} - \frac{1}{L_M} \right) Q_L(z) - \tau \frac{1}{L_M} \left[\alpha_R \frac{\partial T_a}{\partial z} + \alpha_s \frac{\partial T_a}{\partial z} \right] \right\} \end{aligned} \quad (3.9)$$

Noting that the terms within the curly brackets in (3.9) is the ablation a_{ref} at z_{ref} divided by the respective number of days, and assuming a linear approximation, $\tau(z)$ can be calculated from a given $\tau(z_{ref})$ at a reference altitude as

$$\tau(z) = \tau(z_{ref}) + \frac{\partial \tau}{\partial z} \quad (3.10)$$

then equation (3.9) simplifies to

$$\frac{\partial a}{\partial z}\Big|_{z_{ref}} = -\frac{\partial \tau}{\partial z} \left\{ \frac{a_{ref}}{\tau_{ref}} \right\} - \left(\tau(z_{ref}) + \frac{\partial \tau}{\partial z} \right) \frac{1}{L_M} \left[\alpha_R \frac{\partial T_a}{\partial z} + \alpha_s \frac{\partial T_a}{\partial z} \right] \quad (3.11)$$

and the differential of the specific mass balance at z_{ref} is

$$db = \frac{\partial c}{\partial z} dz - \left\{ \frac{\partial \tau}{\partial z} \frac{a_{ref}}{\tau_{ref}} + \left(\tau(z_{ref}) + \frac{\partial \tau}{\partial z} \right) \frac{1}{L_M} \left[\alpha_R \frac{\partial T_a}{\partial z} + \alpha_s \frac{\partial T_a}{\partial z} \right] \right\} dz. \quad (3.12)$$

Note: This equation describes the variation of the specific mass balance with altitude (and thus the mass balance profile) under the assumption that it depends entirely on the vertical gradients of the accumulation, ablation

and air temperature, and the duration of the ablation period. The possible influences of the remaining heat balance key variables and their dependency on the vertical variations of the length of the ablation period are ignored here.

Note: This equation describes the variation of the specific mass balance with altitude (and thus the mass balance profile) under the assumption that it depends entirely on the vertical gradients of the accumulation, ablation and air temperature, and the duration of the ablation period. The possible influences of the remaining heat balance key variables and their dependency on the vertical variations of the length of the ablation period are ignored here.

The vertical mass balance profile in the tropics

The above model was first used on Hintereisferner in Switzerland from climatic data under the assumptions of equilibrium conditions and then compared with a measured profile to form a model for the midlatitudes, with the aim of developing a simple formulation that could be transferred to the postulated climatic differences in the tropical regions.

One of the foremost patterns to note is that the ablation period in tropical regions is assumed $\tau = 365$ days per year everywhere on the glacier and below the z_{ref} (due to the absence of distinct seasons as per the mid to high latitudes (since the fluctuation in seasonal temperature does not exceed the diurnal temperature)). This implies that $\partial\tau/\partial z = 0$, which in turn makes the vertical ablation gradient linear, simplifying equation (3.12) further

$$db = \frac{\partial c}{\partial z} dz - \left\{ \frac{\tau_{ref}}{L_M} \frac{\partial T_a}{\partial z} [\alpha_R + \alpha_s] \right\} dz \quad (3.13)$$

A linear increase with height $\partial c/\partial z = 1 \text{ kg m}^{-2} \text{ m}^{-1}$ is assumed, for altitude zones above the 0° C level. For the Lewis Glacier, $\partial c/\partial z = 2 \text{ kg m}^{-2} \text{ m}^{-1}$ is assumed for altitude zones below the reference line. This value is calculated from observation where $c_{z_{ref}} = 800 \text{ kg m}^{-2}$ and zero 400 m below that level. Ablation gradient is zero above the zero degree (reference) line.

The average values for the parameters used in the model calculation are summarised in the table below:

Table 3.1: Variables and Constants for the calculation of the vertical mass balance gradient of the Lewis Glacier (inner tropics), adapted from Kaser & Osmaston (2002)

Variable	Tropics
$\tau_{z=0}$	365d
$\partial\tau/\partial z$	0 dm ⁻¹
$\partial c/\partial z(z = 0 \uparrow)$	1 kg m ⁻² m ⁻¹
$\partial c/\partial z(z = 0 \downarrow)$	2 kg m ⁻² m ⁻¹
$\partial T_a/\partial z$	-0.0065 K m ⁻¹
T_s (ablation)	273.15 K
T_s (accumulation)	T_a
α_s	1.5 MJ m ⁻² d ⁻¹ K ⁻¹
ε_a	1
ε_s	1
* \Rightarrow • (snow to rain zone)	400 m
σ	4.9×10^{-9} MJ m ⁻² d ⁻¹ K ⁻⁴
L_M	0.334 MJ kg ⁻¹

3.4 Stability and Accuracy

Using Euler's method for discretising the equation (3.13) becomes

$$\Delta b = \frac{\partial c}{\partial z} - \left\{ \frac{\tau_{ref}}{L_M} \frac{\partial T_a}{\partial z} [\alpha_R + \alpha_s] \right\} \Delta z \quad (3.14)$$

The order of accuracy of the Euler scheme is as follows:

- Local error is of the order $O((\Delta z)^2)$;
- Truncation is of the order $O(\Delta z)$; and Global error is of the order $O(\Delta z)$.

Although Euler's method is not very accurate (doubling the number of timesteps only halves the error) and converges slowly, it was deemed suffi-

cient since all the terms in equation 3.13 are linear. A Runge Kutta scheme could be used to discretize the differential if the vertical accumulation gradient is assumed to be non linear or if the scheme is applied to midlatitude glaciers where the ablation term becomes non linear since $\delta\tau/\delta z = 0.1$.

Chapter 4

Results and Analyses

4.1 Modelled Mass Balance Profile of the Lewis Glacier

Specific mass balance of the Lewis Glacier was simulated using temperature profiles from the CRU baseline dataset. As per Figure 4.1, the simulated mass balance profile over the 1961 - 1990 30 year mean was compared to measured observations (red line) taken from 1978 - 1993. The simulated mass balance profile is comparable to the observed mass balance profile since its peaks coincide with those from observed values. However, the actual mass balance values change with different parameter values.

Three parameters, temperature, precipitation and α_s were varied to determine the best model fit to observed data. It was noted that doubling the precipitation (vertical accumulation gradient) overestimated the amount of mass lost by the glacier by approximately 400 kg m^{-2} , all other variables remaining at observed average values (orange line). Setting the value of α_s to 1, the model best simulates the mass balance profile the best when compared to the observed mass balance profile over the 30 year period.

The effect of temperature on the model can best be seen in Figure 4.2. Temperature profiles from the projected climate change scenarios were used in the glacier model. The models predict changes in temperature between 2° K and 4° K with corresponding changes in specific mass balance of 400 kg

m^{-2} and 1200 kg m^{-2} when compared with the baseline profile (top line).

4.2 Mass Balance and Volume of Glacier

Having determined the optimum parameter values for the model, the volume of the glacier was determined by multiplying the specific mass balance at each elevation band with the corresponding area that the glacier occupied at that level. However, the area occupied by the glacier can only be inferred from observation. At present, there is no way of predicting the area occupied by a glacier in the future apart from statistical inference of present data.

The observed area covered by the glacier was used to project when the glacier would cease to exist using linear regression. It was assumed that the area of the glacier would continue to decrease since the model predicts negative mass balance trends. As suggested by Figure 4.3, the Lewis Glacier will cease to exist in 2039 if the linear regression line is used to predict future changes in area of the glacier.

The relationship between specific mass balance, meltwater and area of the Lewis Glacier is summarised in Figure 4.4. The volume of the glacier is directly proportional to the potential runoff from the glacier. Negative mass balance coupled with decreasing area of the glacier implies that meltwater from the glacier also decreases.

4.3 Implications of Surface Runoff and Glacier Melt

To analyse the implications of glacier meltwater downstream from the glacier, average annual runoff from the hydrological model for the grid cell was added to the meltwater and then divided by 2000 km^2 to get the runoff per square km. The Lewis Glacier has a south east aspect and average annual runoff from 8 grid cells adjacent to the east, south and south east of Mount Kenya grid cell were used to analyse the effect of the glacier downstream.

It is clear from the figures above, that as the size of the catchment is increased, the impact of the glacier on runoff generation decreases. Infact, it

has little effect on the runoff from baseline 1961 - 1990 data and no effect on runoff for projected climate change scenario using 2010 - 2039 IPSL data (Figure 4.6).

The glacier presently occupies 0.31 km², which accounts for 0.0155% of the grid cell. As per the analyses above, this area is projected to decrease even further and hence runoff generated from the meltwater of the glacier has little effect on the catchment area. As per Figures 4.5 and 4.6 below, it can be seen that as the size of the catchment is increased, the meltwater from the glacier has no impact on the runoff generated in adjacent grid cells.

4.4 Climate variability and Runoff

From the above analyses, it was noted that the Lewis Glacier has little or no effect on average annual runoff. The following figures show changes to runoff in Kenya due to climate variability using the 5 models, CCMA CGCM31, IPSL CM4, MPI ECHAM5, UKMO HADCM3, and NCAR CCM30 which are based on IPCC SRES emission scenario A1B for the years 2040 - 2069.

Figure 4.7 shows the average annual runoff between 1961 and 1990. It shows higher runoff in the Rift Valley, Central Kenya, West Kenya and the Coast. Average runoff in the North and North East of the country is less than half of that in other parts. The model shows that there is highest runoff in the Mount Kenya region.

The CCMA CGCM31 model shows the highest increase in average runoff by 105% for most parts of Kenya and in particular the Rift Valley Region. In contrast, the MPI ECHAM5 model simulates decrease in runoff in Western Kenya by 15% and an increase in runoff in Eastern Kenya. All the models show a decrease in runoff at the coast between 5 and 15% except NCAR CCM30.

This bodes well for agricultural sector since tea and coffee farms are located in the highlands (Central Kenya) and horticultural farms are located in the Rift Valley.

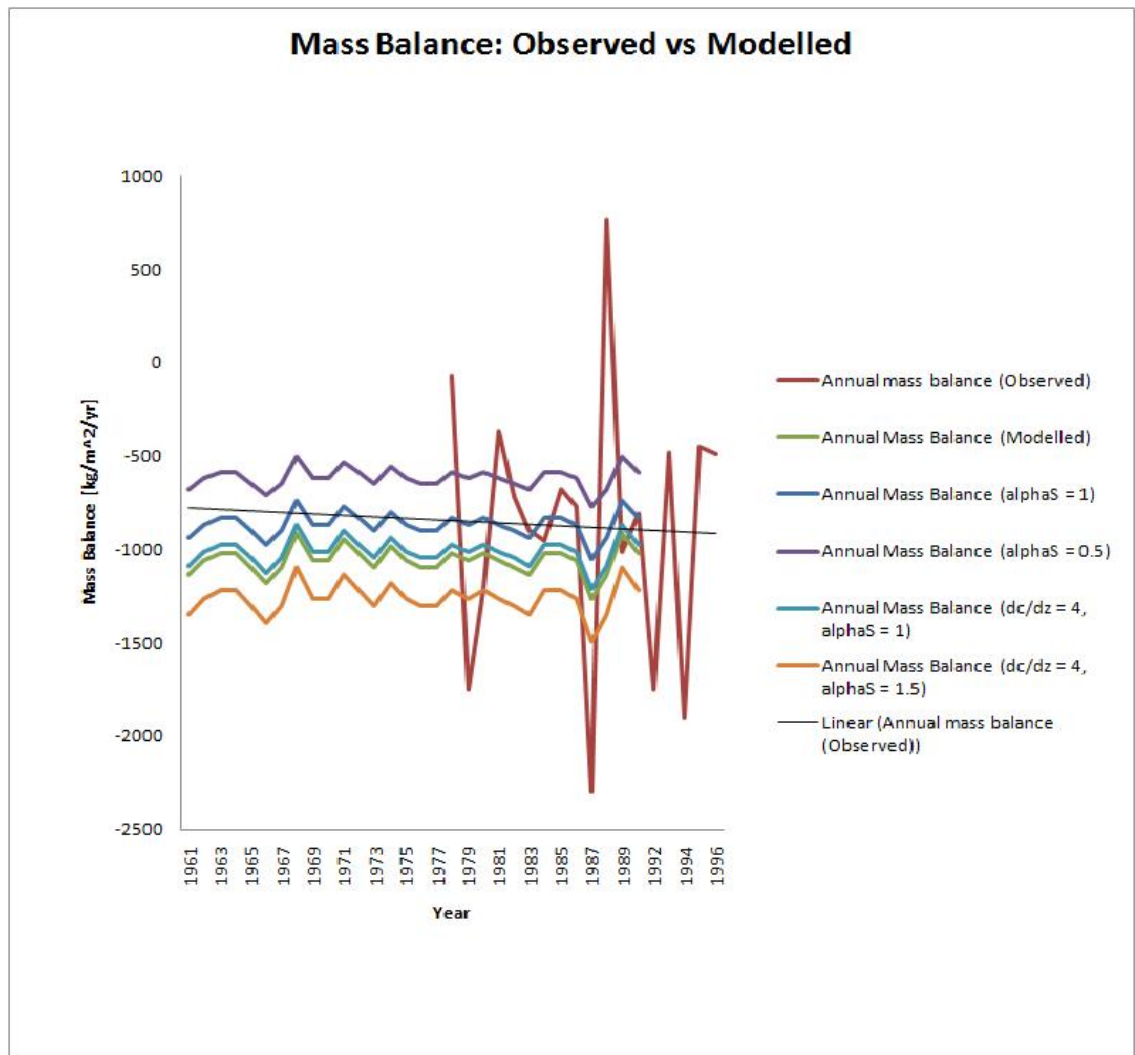


Figure 4.1: Observed and simulated mass balance profiles.

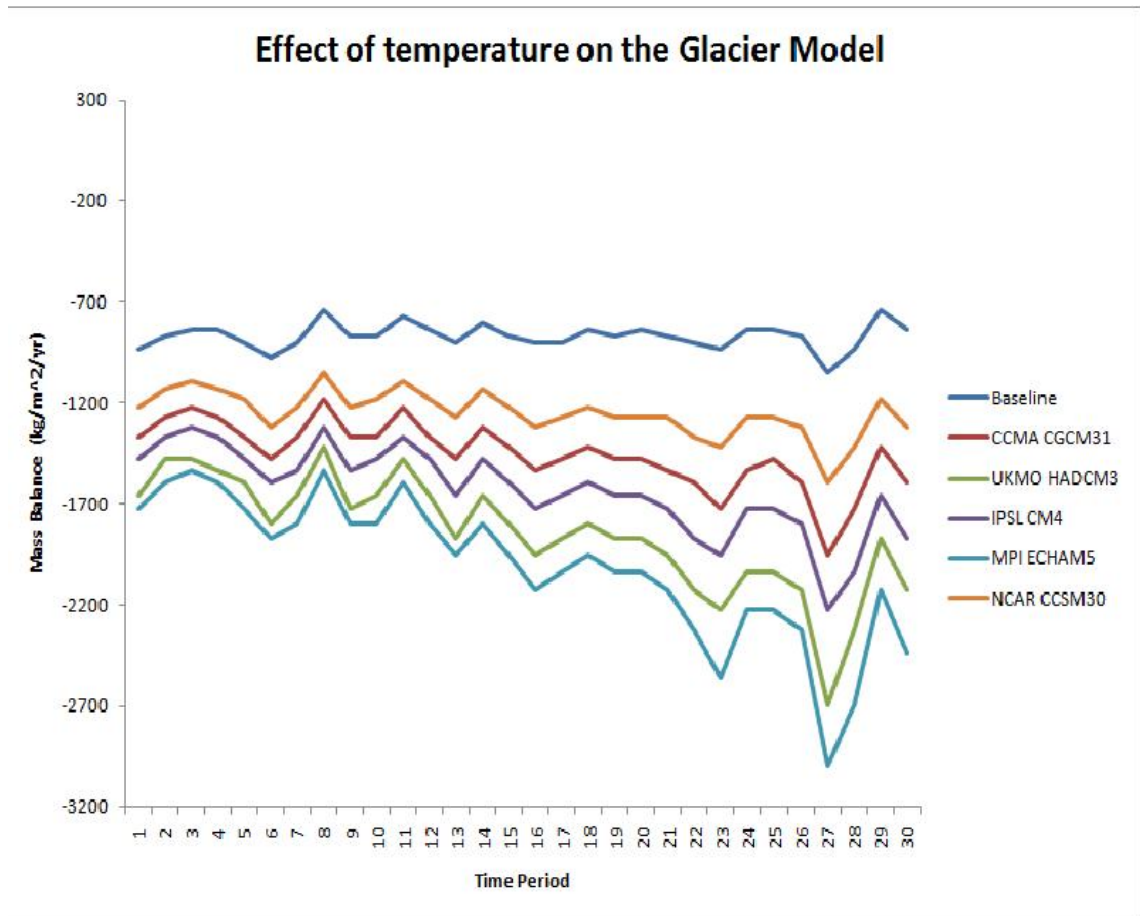


Figure 4.2: Specific mass balance profile simulations with different climate change projections.

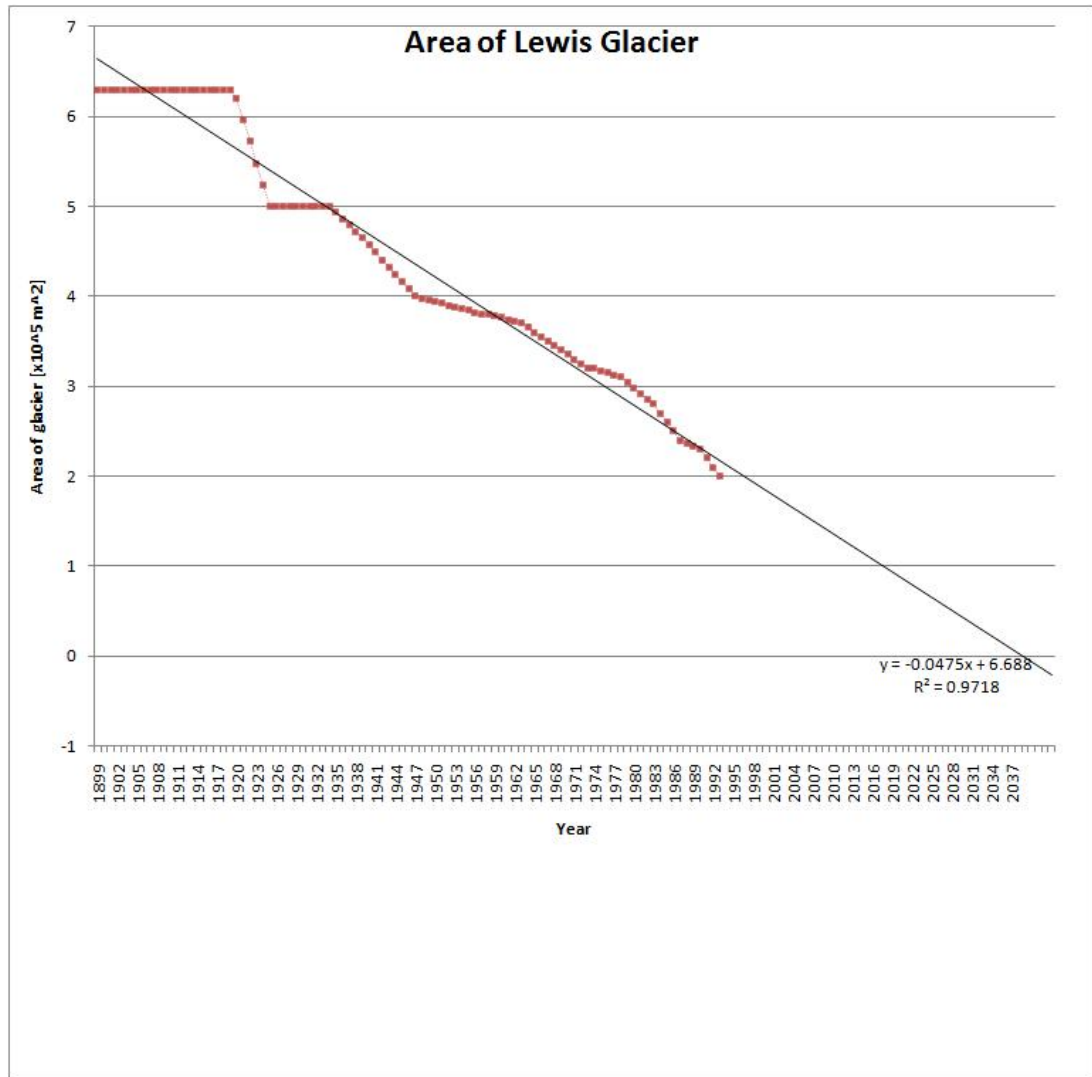


Figure 4.3: Projected area of Lewis Glacier over time.

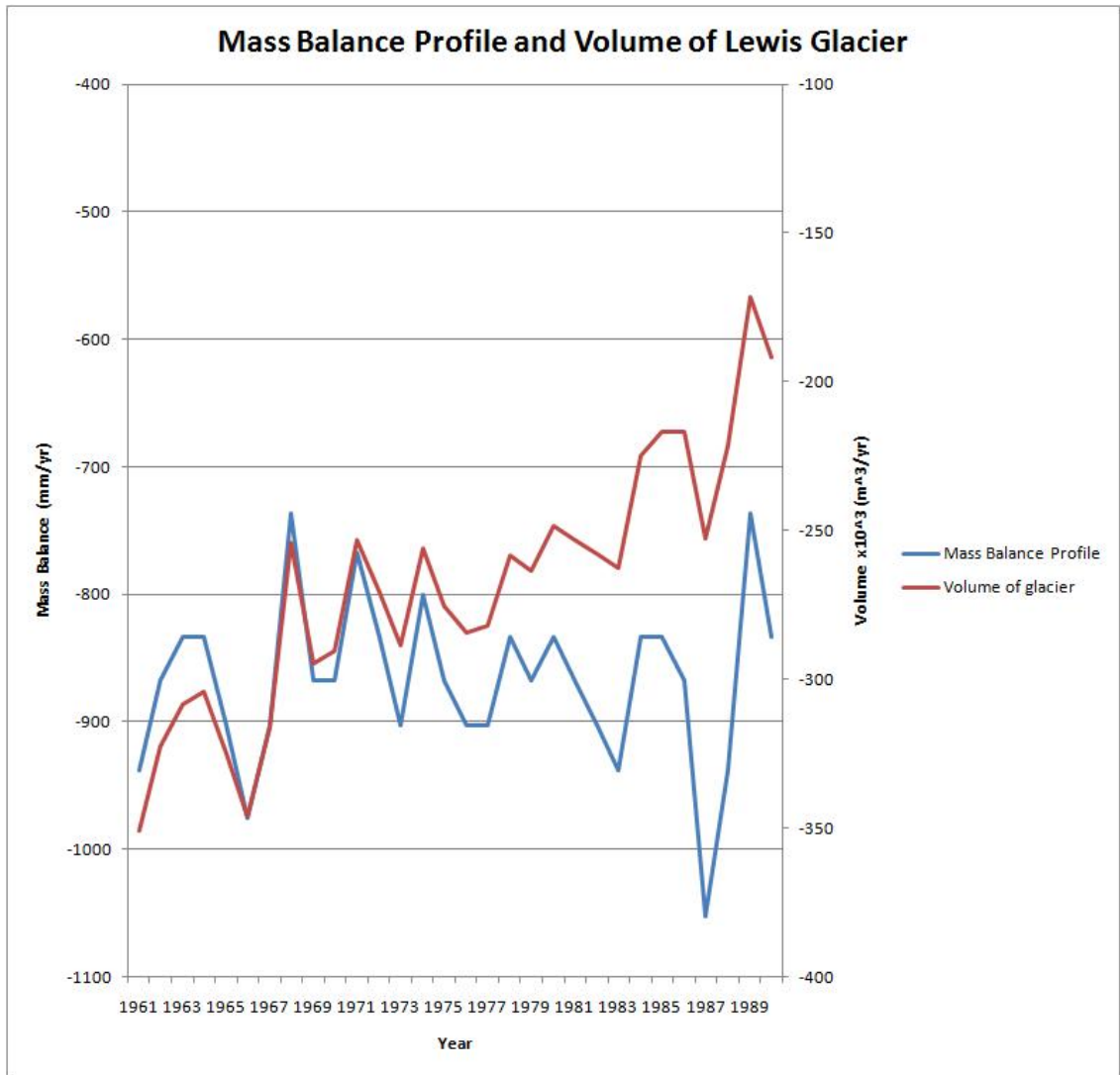


Figure 4.4: Change in volume of glacier.

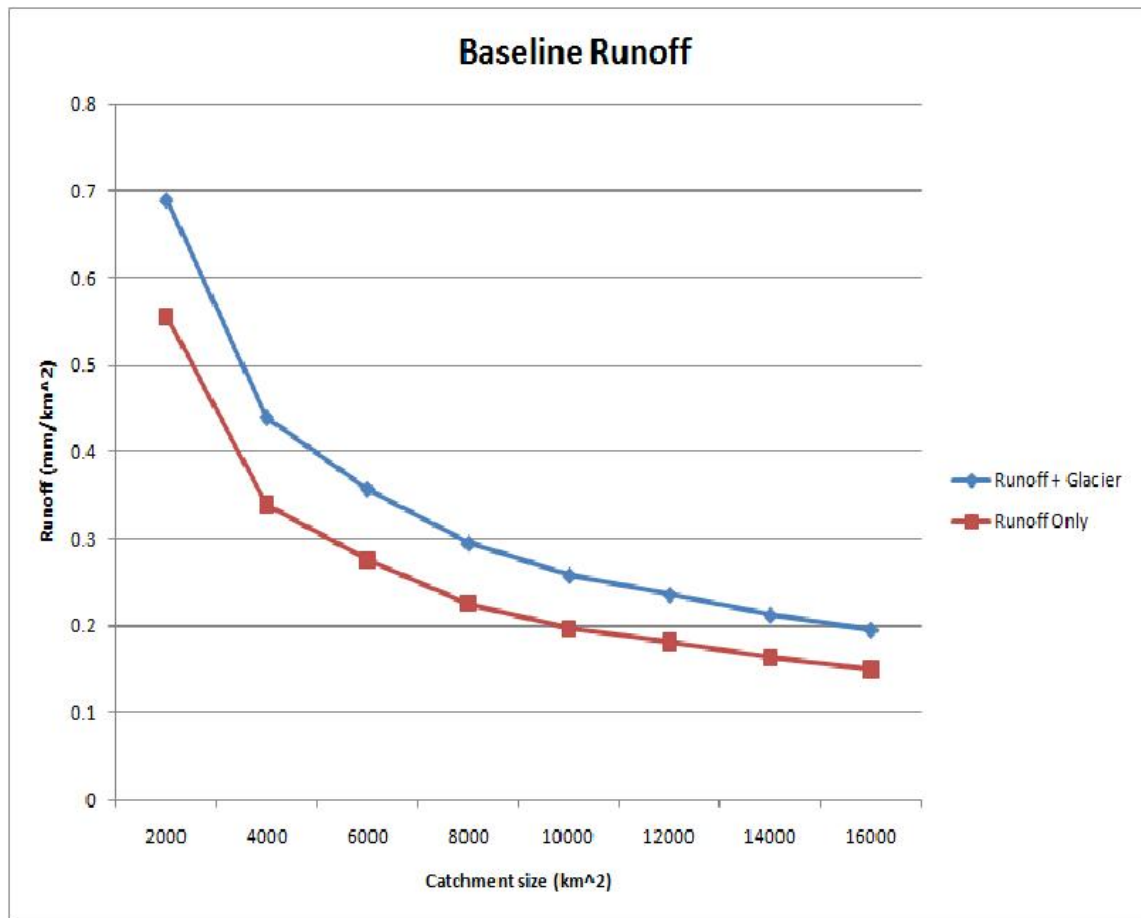


Figure 4.5: Effect of glacier on runoff and surrounding catchment for current climate.

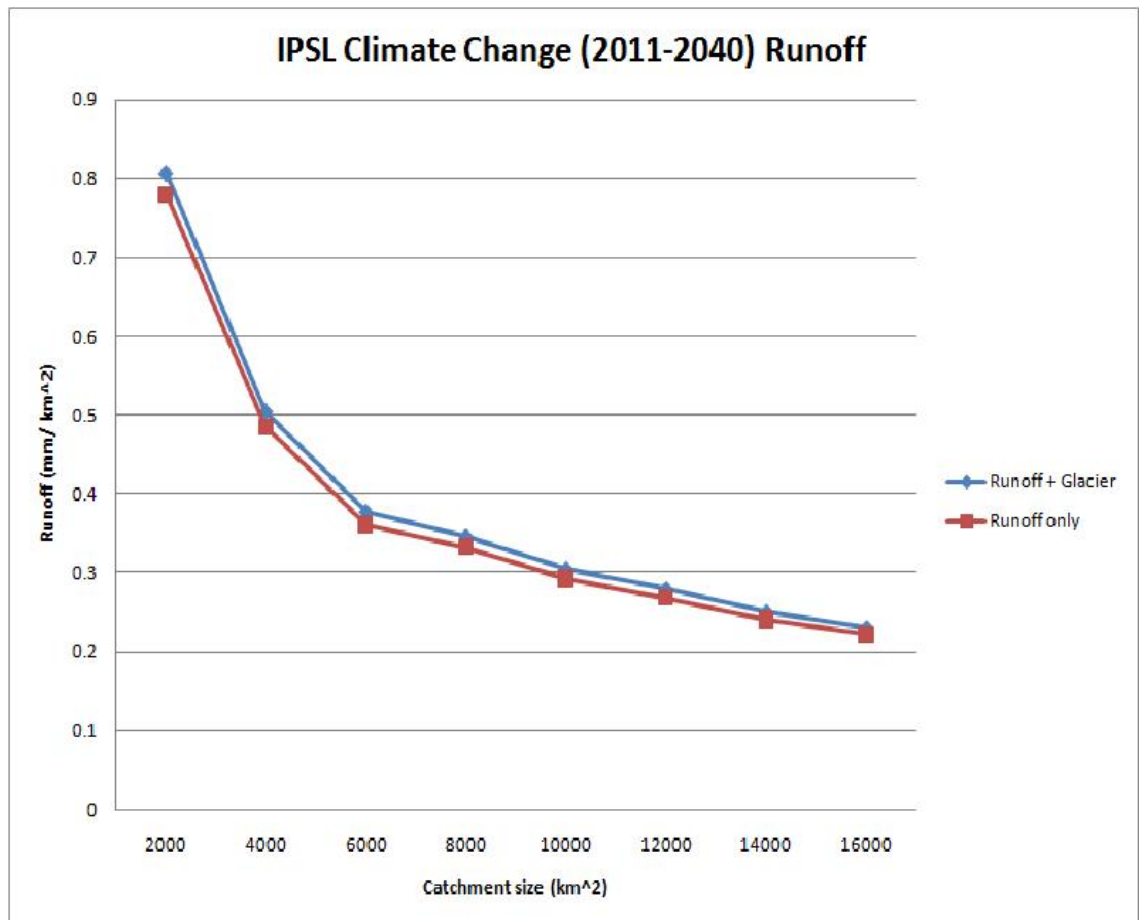


Figure 4.6: Effect of glacier on runoff and surrounding catchment for future climate.

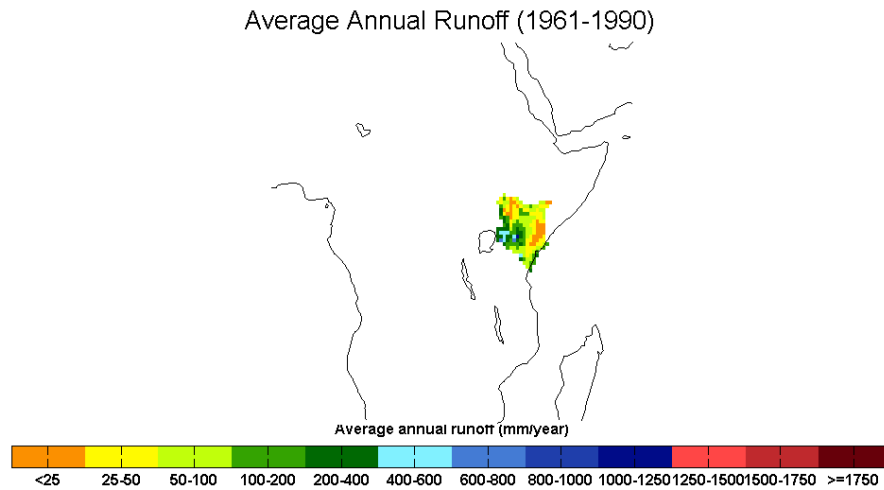


Figure 4.7: Average annual runoff simulation for baseline data (1961 - 1990).

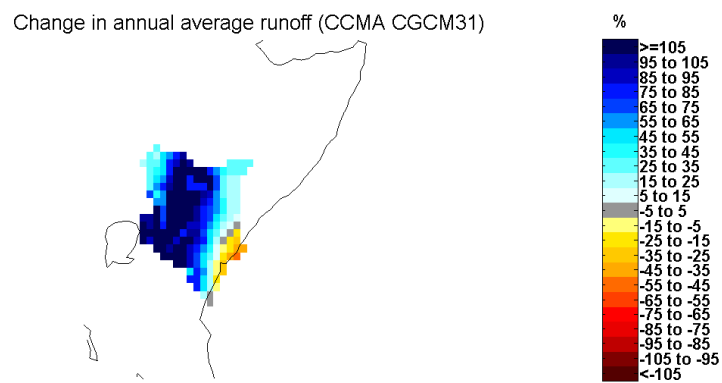


Figure 4.8: Percentage change in annual average runoff for CCMA CGCM31 model.

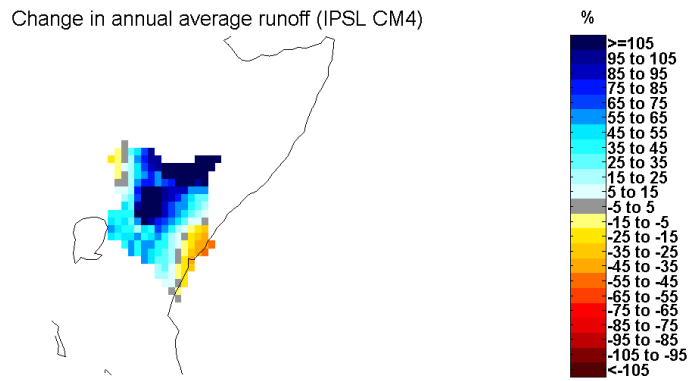


Figure 4.9: Percentage change in annual average runoff for IPSL CM4 model.

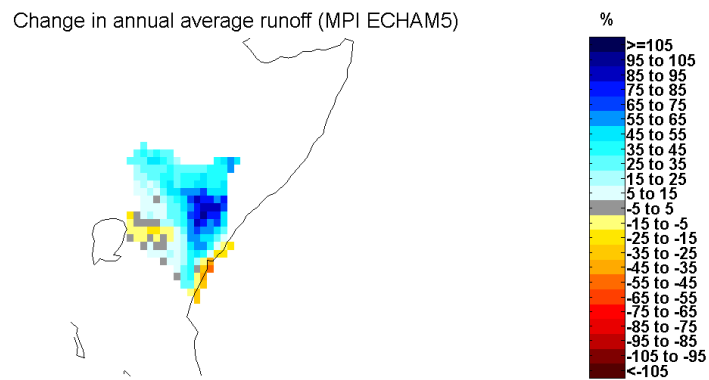


Figure 4.10: Percentage change in annual average runoff for MPI ECHAM5 model.

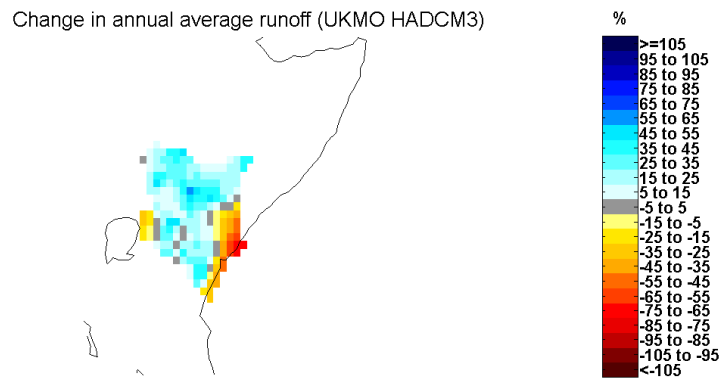


Figure 4.11: Percentage change in annual average runoff for UKMO HADCM3 model.

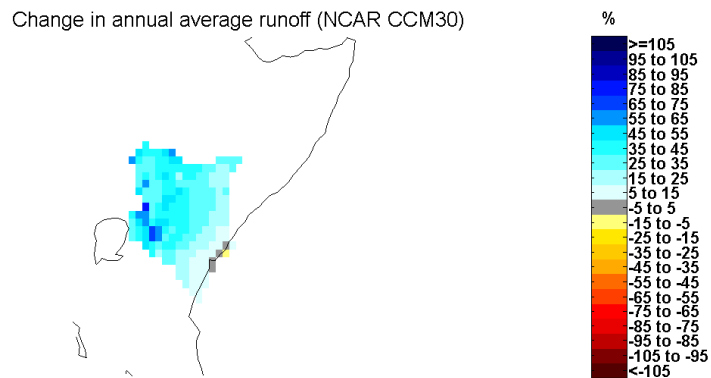


Figure 4.12: Percentage change in annual average runoff for NCAR CCM30 model.

Chapter 5

Discussion and Summary

5.1 Caveats

Caveats are associated with all components of the study - the glacier model, the hydrological model, and in climate variability projections.

One of the key limitations of all the models is that estimation of current and future mass balance profiles and runoff is based on simulated data and not on observations. Therefore, any bias in the simulation model will lead to a bias in the projected changes (Arnell, 2004).

The glacier model does not simulate the specific mass balance to the correct amplitude. However, the simulations do model the longterm average reasonably well as discussed earlier. This could be further investigated by validating the model against other tropical glaciers. Another caveat is predicting the area covered by the glacier so as to determine the volume (in water equivalent) stored by the glacier.

Although Euler's method is not very accurate (doubling the number of timesteps only halves the error) and converges slowly, it was deemed sufficient since all the terms in equation 3.13 are linear. A Runge Kutta scheme could be used to discretize the differential if the vertical accumulation gradient is assumed to be non linear or if the scheme is applied to midlatitude glaciers where the ablation term becomes non linear since $\delta\tau/\delta z = 0.1$.

It is assumed that all the water in the glacier will become meltwater and

hence runoff. Interception by vegetation, soil texture and evaporation have been ignored. This would reduce the runoff generated due to meltwater even further.

The hydrological model form and parameterisation is influenced and constrained by the availability of input data. Data sets used in the modelling are gridded at different spatial resolution and some information is lost along the way as it is interpolated down to the $0.5^\circ \times 0.5^\circ$ resolution used in the hydrological model.

Uncertainty in hydrological projections arises from several sources:

- Internal climate variability
- Emissions uncertainty
- Climate model uncertainty
- Simplification of processes, e.g. vegetation feedbacks, aerosols
- Downscaling and hydrological model uncertainty (Stott *et al.*, 2008)

5.2 Conclusion

From the analysis carried out in Chapter 4, it can be concluded that the Lewis Glacier is retreating at a relatively fast rate, the main factor driving it being temperature. The area covered by the glacier will all but disappear by 2039 if the current rate of decrease of 4.5% is kept up. Glaciers have been known to retreat faster than has been predicted as per the IPCC 1997 and 2002 reports.

Furthermore, the glacier represents 0.0155% of the grid cell and thus has little to no contribution to the streamflow of the region. However, using climate change projections from 5 models based on A1B IPCC SRES emissions, the Mac-PDM model predicts increased runoff in Kenya. More than 105% increase in some areas such as parts of the Rift Valley, Western and Central Kenya are predicted while the North East and Eastern parts of Kenya

may also see an increase in runoff which may relieve stress on the people living in this semi-arid region at present.

5.3 Further Work

Due to time constraints and problems encountered during the study, the following work could not be investigated but would add value to the study::

- Extend the simulations to other tropical glaciers and the effect of climate variability on runoff from glacier melt;
- Develop a method to predict the change in the area covered by the glacier based on physical concepts; and
- Incorporate the glacier model into the hydrological model to account for glacier meltwater contributions to streamflow at the global level;

Other investigations could be based on the socio-economic impacts of melting of tropical and other glaciers, including changes in sea level.

Bibliography

- [1] Arnell, N.W.(1999a) A simple water balance model for the simulation of streamflow over a large geographic domain, *Journal of Hydrology*, **217**, pp. 314–335.
- [2] Arnell, N.W. (1999b) The effect of climate change on hydrological regimes in Europe: a continental perspective, *Global Environmental Change*, **9**, pp. 5–23.
- [3] Arnell, N.W. (2003) Effect of IPCC SRES emission scenarios on river runoff: a global perspective, *Hydrology and Earth System Science*, **7**, pp. 619–641.
- [4] Arnell, N.W. (2004) Climate change and global water resources: SRES emission and socio-economic scenarios, *Global Environmental Change*, **14**, pp. 31–52.
- [5] Bienn, D.I. and Evans, D.J.A (1998) *Glaciers and Glaciation*, Arnold, London.
- [6] ClimGen <http://www.cru.uea.ac.uk/~timo/climgen/>, climatic Research Unit, (checked on 13.08.2009).
- [7] Hastenrath, S. (1995) Glacier Recession on Mount Kenya in the context of global tropics, *Bull. Inst. fr. etudes andines*, [Electronic], **24**(3), pp. 633–638. Available: [http://www.ifeanet.org/publicaciones/boletines/24\(3\)/633.pdf](http://www.ifeanet.org/publicaciones/boletines/24(3)/633.pdf), (last checked on 15.08.2009).

- [8] Hock, R. (2005) Glacier melt: a review of processes and their modelling, *Progress in Physical Geography*, **29**, pp. 362–391.
- [9] Innes, P. (2009) *Tropical Weather Systems lecture notes*
- [10] IPCC (2001) Climate Change 2001: Working Group I: The Scientific Basis [electronic] [http://www.grida.no/publications/other/ipcc_tar/?src = /CLIMATE/IPCC_TAR/WG1/029.htm](http://www.grida.no/publications/other/ipcc_tar/?src=/CLIMATE/IPCC_TAR/WG1/029.htm) (checked 21.08.2009) Karlen, W., Fastook, J.L., E. 6000 Cal. Years B.P: Implications for Holocene Climatic Change in East Africa *Ambio*, pp. 409–418.
- [11] Kaser, G. (2001) Glacier–Climate Interaction at Low Latitudes, *Journal of Glaciology*, **47**, pp 195–204.
- [12] Kaser, G and Osmaston, H. (2002) *Tropical Glaciers*, Cambridge University Press.
- [13] Kuhn, M. (1980) Climate and Glaciers. Sea level, ice and climatic change. (Proceedings of the Canberra Symposium, Dec 1979), *IAHS Publication Number*, **131**, 3–20. In Kaser, G and Osmaston, H. *Tropical Glaciers*, Cambridge University Press, 2002.
- [14] Ohmura, A. (2001) Physical Basis for the Temperature-Based Melt Index Method, *Journal of Applied Meteorology*, **40**, pp. 753–761.
- [15] Stott, P. (2008) Observed and projected changes in climate as they relate to water; Workshop on IPCC AR4 at Bonn Climate Change Talks - UNFCCC SBSTA 28th Session - Bonn, Germany, 6 June 2008 [electronic] URL: <http://www.ipcc.ch/pdf/presentations/briefing-bonn-2008-06/observed-project>
- [16] Schaeffi, B., Hingray, B., Niggli, M., and A. Musy (2005) A conceptual glacio-hydrological model for high mountainous catchments *Hydrology and Earth System Sciences*, **9**, pp. 95–105.

- [18] <http://www.wri.org/publications/>, World Resources Institute, (checked on 13.07.2009).
- [19] Young, J. A. T and Hastenrath, S. (1991) Glaciers of the Middle East and Africa—Glaciers of Africa. Satellite Image Atlas of Glaciers of the World *US Geological Survey Professional Paper*, **1386-G-3**, G49–G70. In Karlen, W., Fastook, J.L., Holmgren, K., Malmstrom, M., Matthews, J. A., Odada, E., Risberg, J., Rosqvist, G., Sandgren, P., Shemesh, A., and Westerberg, L. (1999) Glacier Fluctuations on Mount Kenya since ~ 6000 Cal. Years B.P: Implications for Holocene Climatic Change in East Africa *Ambio*, pp. 409–418.